BRNO UNIVERSITY OF TECHNOLOGY
FACULTY OF ELECTRICAL ENGINEERING AND COMPUTER SCIENCE
DEPARTMENT OF CONTROL AND INSTRUMENTATION

Ing. Petr Blaha

COULOMB FRICTION IDENTIFICATION USING HARMONIC BALANCE METHOD OF TWO RELAY SYSTEM

ODHAD SUCHÉHO TŘENÍ POUŽITÍM METODY HARMONICKÉ LINEARIZACE SYSTÉMU SE DVĚMA NELINEARITAMI TYPU RELÉ

PhD Thesis

Teze doktorské disertační práce

Doctoral study program: Cybernetics and Informatics

Supervisor: Prof. Ing. Petr PIVOŇKA, CSc.

Reviewers: Prof. Ing. Vladimír Bobál, CSc.
Prof. Ing. Mikuláš Alexík, CSc.

Date of PhD thesis defence: 6. June 2001

Contents

1. INTRODUCTION

The presence of nonlinear component in controlled system usually brings together the difficulties in control algorithm design. It disallows the usage of classical methods that are widely used in linear systems. To solve this problem, it is necessary either to clear away the parasitic behavior of the nonlinearity or to use specialized and often more complex designing methods. One of the problematic nonlinearities, which is of our interest in this work, is mechanical friction. It represents typical contradiction in human beings everyday life. It is in some cases highly desirable (walking, brakes, etc.) but in other cases it acts adversely (wearing, temperature increase, energy losses, etc.).

The mechanical friction is complex physical phenomenon, which also influences the control performance. The presence of friction in controlled system often gives rise to limit cycles around the reference position (so called "hunting effect") or to steady state error. It was observed that the limit cycles under relay feedback are affected by the presence of friction and could, in this way, help us to estimate Coulomb friction. For derivation of algorithm for friction estimation we consider the friction having relay character - i.e. the friction acquires two possible values $\pm f$ depending on the velocity sign (Coulomb friction). Consequently, we were led to study linear systems influenced by two relays as particular physical system. The main advantages of such an approach - friction estimation under relay feedback – are the clarity and simplicity of the mathematical tools and the closed loop context which ensures the system operation in desired range of output values. The latter property is important e.g. for the systems containing a pure integrator which is the case of waste majority of position control systems.

Friction estimation is particularly useful for the precise position control that is achieved, unlike the purely linear design, by adding a friction compensator to the system. The friction compensation may be realized in different ways.

We should be able to model the friction as precisely as possible for the model-based friction compensation techniques to be efficient (danger of overcompensation [51]). Often an adaptive implementation is needed to cope with the time-variance of friction parameters (see [16], [7] and [27]).

Our approach of Coulomb friction estimation can represent the first (and very important) stage of such an adaptive scheme, aiming to find initial estimates for the further adaptation. In addition, in some classes of systems, even the application of a simplified friction model based compensator (the Coulomb model in our case) can considerably improve the control performance (see [3]).

2. OBJECTIVES

The majority of friction models use Coulomb friction as a key component. Coulomb friction is included not only in static but also in dynamic models. There exists big amount of methods, which attempt to find more or less complicated model

of friction. The problem is that they usually require some additional knowledge about the system, which is influenced by friction. This thesis tries to find an algorithm for Coulomb friction estimation with no additional information about the system. The goal of this thesis is to:

1. analyze the two-relay system in time domain.

2. specify the describing function of equivalent nonlinearity and analyze the influence of parameters changes.

3. discuss the problematic of existence and stability of limit cycle oscillations

4. find algorithm for Coulomb friction estimation using harmonic balance method.

5. prove the correctness of proposed algorithm in simulations.

6. describe the influence of more complicated model than Coulomb friction model on precision of the proposed algorithm.

7. show real-time application of presented algorithm.

8. point out the negative influence of friction on point of frequency response measurement according to PID controller adjustment using relay experiment.

3. METHODES

3.1. Time Domain Analysis

- Description of the two-relay system using switching instant conditions and switching direction conditions (as in [45]). It allows to simulate the behavior of this system and it also enables to mathematically describe the condition of no additional switching.
- Phase plane analysis (see [44] and [50]) – it enables to analyze the behavior of second order system. It gives inside into existence and stability of limit cycles (Poincaré-Bendinxon theorem).

3.2. Frequency Domain Analysis

- First harmonic approximation – it is used to designate the describing function of equivalent nonlinearity.
- Extended Nyquist criteria of stability – is employed to prove the existence and the stability of limit cycles
- Harmonic balance method – is used to study the influence of outer relay parameter changes on frequency of limit cycle oscillations. Afterwards, it is helpful for equation and algorithm derivation for Coulomb friction estimation.
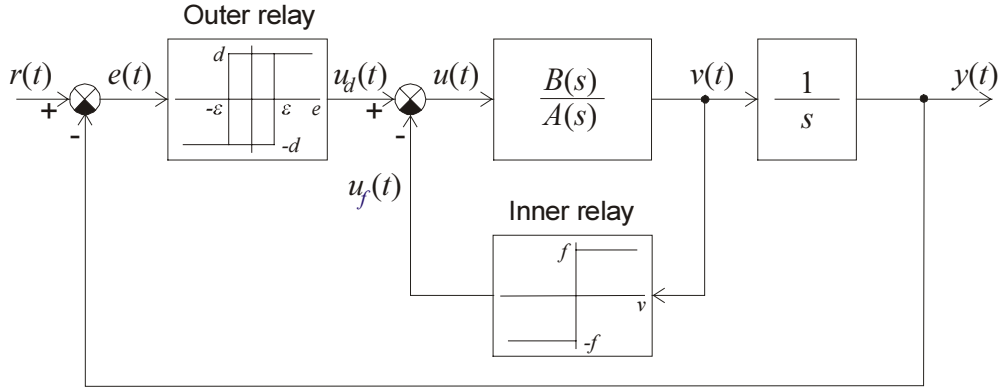
4. MAIN RESULTS

4.1. Two-Relay System

Figure 1: Feedback system structure

An underlying system studied in this thesis is shown in Figure 1. This system contains besides a stable linear part $B(s)/A(s)$ followed by an integrator $1/s$ also two relay nonlinearities (two-relay system). The inner relay with amplitude f is modeling the Coulomb friction and the outer relay with amplitude d and with hysteresis ε is ensuring the position feedback. The linear part of the system is described by the transfer function

$$G(s) = \frac{B(s)}{sA(s)} = \frac{b_m s^m + \ldots + b_0 s^0}{s(a_n s^n + \ldots + a_0 s^0)} \qquad b_0 \neq 0 \qquad (4.1)$$

It is not necessary to care about the viscous friction for system layout in Figure 1 because in the case of non-zero viscous friction it is possible to include this phenomenon into the linear part $B(s)/A(s)$ due to its linear character. The linear part then changes to

$$\frac{B'(s)}{A'(s)} = \frac{B(s)}{A(s) + F_v \cdot B(s)} \qquad (4.2)$$

where F_v is the coefficient of viscous friction.

4.1.1. Transient Response

The behavior of both relays can be described by switching instants conditions and by switching direction conditions [45]. The switching instants condition defines the time of relay switches. The switches are good provided that the direction of the motion remains the same at the switching instant. Switching instants for both, outer and inner relays are given as follows:

Outer relay switching instants: they appear at a time when $e(t) = r - y(t)$ crosses the hysteresis value ε (assuming that $\dot{y}(t_0') < 0$).

$$\begin{cases} r - y(t_k') = (-1)^k \varepsilon & \ldots \text{switching instants conditions} \\ (-1)^k \dot{y}(t_k') < 0 & \ldots \text{switching direction conditions} \end{cases}$$

where t'_k ($k = 0, 1, 2, \dots$) denotes the outer relay switching instants.

Inner relay switching instants: they appear at a time when $\dot{y}(t)$ changes its sign.

$$\begin{cases} \dot{y}(t_k) = 0 & \dots \text{switching instants conditions} \\ (-1)^k \ddot{y}(t_k) > 0 & \dots \text{switching direction conditions} \end{cases}$$

(4.4)

where t_k ($k = 0, 1, 2, \dots$) denotes the inner relay switching instants.

This study is restricted to the case of simple oscillations. The mathematical relation describing simple oscillations is expressible with a set of equations

$$\begin{cases} (-1)^{k+1}[r - y(t)] < \varepsilon & \text{for } t'_k < t < t'_{k+1} \\ (-1)^{k+1} \dot{y}(t) < 0 & \text{for } t_k < t < t_{k+1} \\ t'_k \leq t_k < t'_{k+1} \leq t_{k+1} \end{cases}$$

(4.5)

The set of equations (4.5) is also called condition of no additional switching. It says that one switch of relay is followed by one and only one switch of the other relay and vice versa. The following mathematical description of the two-relay system can be used to compute the system's output $y(t)$ for any given time instant. Let's assume initial conditions

$$\underbrace{u_d(t) = -d \quad e(t) < \varepsilon}_{\text{for outer relay}} \qquad \underbrace{\dot{y}(t) < 0}_{\text{for inner relay}} \qquad \text{where } t = 0$$

The considered feedback system can be replaced with interconnection of linear part $G(s)$ with step response $h(t)$ and one nonlinear part described by $u(t) = u_d(t) - u_f(t)$. The validity of switching conditions (4.3)-(4.5) enables us to write equation describing transient behavior of the system as

$$y(t) = (-d + f)h(t) + 2 \sum_{k=0}^{\infty} (-1)^k [d \cdot h(t - t'_k) - f \cdot h(t - t_k)] + y_{nc}(t)$$

(4.6)

where $y_{nc}(t)$ is the natural component of transient response given by non-zero initial state.

In the case of steady state limit cycles, the additional condition can be added defining the fact that the time periods between the two successive switches of each relay are constant.

In the case of stable and symmetrical limit cycle, the basic structure of underlying system in Figure 1 can be substituted by simpler scheme, which can be seen in Figure 2. This scheme is more advantageous for frequency domain analysis since it enables us to use harmonic balance method. Both relays are replaced there with one nonlinearity with equivalent behavior – equivalent nonlinearity. The presence of the integrator in transfer function $G(s)$ causes that no DC component propagates through the equivalent nonlinearity even for the case $r(t) = const. \neq 0$. This fact is necessary assumption for harmonic balance method usage.
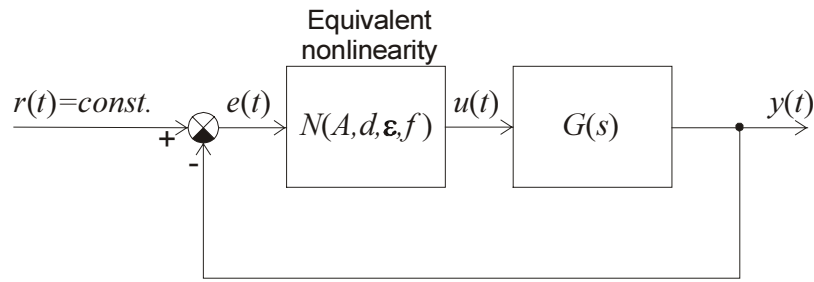
Figure 2: Equivalent feedback system

4.1.2. Phase Plane Analysis

Phase plane analysis is a simple graphical method for studying second-order systems. Since it is the graphical method, it gives advantage of good physical inside into system behavior. Another advantage is that it does not fail to work with the systems containing *hard nonlinearities* (as it is in our case). The hard nonlinearity is the one that does not allow linear approximation. Phase plane analysis can be used to solve motion trajectories for various initial conditions, for stability decision and for limit cycles detection. This method is limited in its usage for systems up to second order inclusive because the study of higher-order systems is graphically complex. The phase planes generated using method of isoclines for different settings of linear part $G(s)$ and of both relays are not presented there due to lack of space. Only principal results are mentioned as follow.

- Some systems converge to limit cycles faster than the others. With the convergence speed we mean number of limit cycle periods needed to reach the steady state oscillations.
- The linear part must be stable to obtain stable limit cycles.
- The outer relay amplitude d must be always higher than inner relay amplitude f. This limitation is natural. Otherwise the limit cycles are not generated because they are broken with friction.
- Hysteresis of outer relay must be nonzero to guarantee the existence of limit cycles for second order linear part $G(s)$. This condition is not necessary for linear parts of higher order.

4.2. Equivalent Nonlinearity

4.2.1. Response to Harmonic Signal

The response of equivalent nonlinearity to a harmonic input signal $e(t) = A \cdot \sin(\omega t)$ is composed of two rectangular signals $u_d(t)$ and $u_f(t)$ which are mutually shifted and which correspond to the outer and the inner relay output, respectively (see Figure 3).

Their phase shift, according to the sinusoidal input signal $e(t)$, is caused by:

- presence of the hysteresis ε in the outer relay,

- dependency of the inner relay output on the velocity $\dot{y} \equiv -\dot{e}$

The outer relay produces phase shift that depends on the amplitude A of the sinusoidal input signal and on the value of the hysteresis ε $\alpha_1 = \arcsin(\varepsilon/A)$.
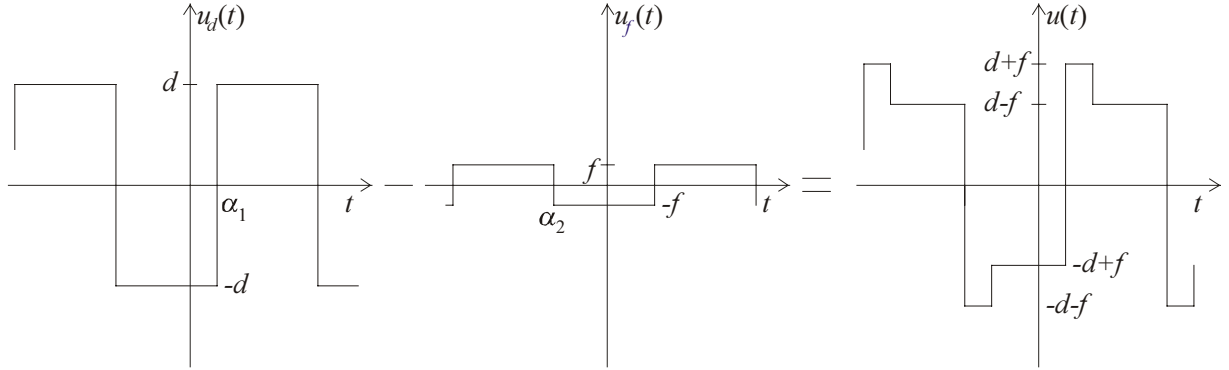
Figure 3: The output signal of equivalent nonlinearity

The velocity feedback of the inner relay gives a phase shift $\alpha_2 = \pi/2$, which is the phase shift between the output y and its derivative $\dot{y} = v$. The resulting phase shift between the signals $u_d(t)$ and $u_f(t)$ is given by the sum of both phase shifts $\alpha = \alpha_1 + \alpha_2$.

4.2.2. Describing Function

The describing function of the equivalent nonlinearity $N(A, d, \varepsilon, f)$ is determined as a parallel combination (i.e. a sum) of two describing functions of the two relays with amplitude d and f with the phase shifts explained above.

$$N(A, d, \varepsilon, f) = \frac{4}{\pi A}\left(d \cdot e^{-j \cdot \alpha_1} - f \cdot e^{-j \cdot \alpha_2}\right) = \frac{4}{\pi A}\left(d \cdot e^{-j \cdot \arcsin\frac{\varepsilon}{A}} + f \cdot e^{j \cdot \frac{\pi}{2}}\right) \quad (4.7)$$

One can notice that the equation (4.7) depends on four parameters. Following section shows the dependency on variations in d and ε.

4.2.3. Analysis of Limit Cycles

This section gives the discussion on the influence of the outer relay parameters on limit cycle frequency evolution. This essential issue will be further used in the proposed method for inner relay amplitude identification (section 4.3). The harmonic balance method uses the graphical interpretation of condition of harmonic balance

$$G(j\omega) = \frac{-1}{N(A, d, \varepsilon, f)} \quad (4.8)$$

This equation graphically represents the intersection between the Nyquist plot of linear part $G(j\omega)$ and the plot of negative inverse of describing function $-1/N(A, d, \varepsilon, f)$.

First, let's consider the limit case when the hysteresis is not included in the outer relay ($\varepsilon = 0$). The negative inverse of $N(A, d, f)$ is then described by

$$\frac{-1}{N(A,d,f)} = \frac{-\pi A}{4}\left(\frac{d - j \cdot f}{d^2 + f^2}\right) \tag{4.9}$$

The plot of this function (as a function of output amplitude A) is represented by straight lines starting in point (0,0) and having the slopes dependent on the ratio between the relay amplitudes d and f. Because the inner relay amplitude f is fixed,
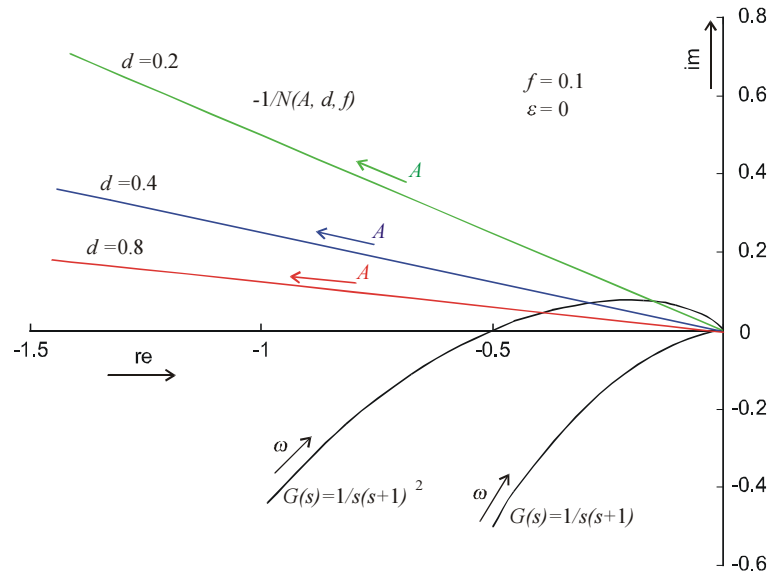

Figure 4: Intersection between the frequency characteristic of $G(s)$ and the function $-1/N(A,d,f)$ for three different outer relay amplitudes without hysteresis.

it is meaningful to investigate only the influence of changes in the outer relay amplitude d. The qualitative graph representing negative inverse of $N(A,d,f)$ is depicted in Figure 4. An increase of d implies an increase of the angle between the straight line and the positive real axis. This straight line lies in second quadrant for all values of d.

Depending on the linear part characteristics, the phase modification induced by the modification of d will be equivalent to a frequency of limit cycles modification.

The formula (4.9) becomes more complicated for the outer relay with hysteresis ε

$$\frac{-1}{N(A,d,f)} = \frac{-\pi A}{4}\left(\frac{\sqrt{1 - \dfrac{\varepsilon^2}{A^2}} - j \cdot \left(\dfrac{f}{d} - \dfrac{\varepsilon}{A}\right)}{1 - \dfrac{2f\varepsilon}{dA} + \dfrac{f^2}{d^2}}\right) \tag{4.10}$$

We can study the influence of changing the values of outer relay amplitude d and hysteresis ε. The loci of $-1/N(A,d,\varepsilon,f)$ of equivalent nonlinearity, when the outer relay includes a constant hysteresis ($\varepsilon = const.$), is shown in Figure 5 for three different values of outer relay amplitude d.
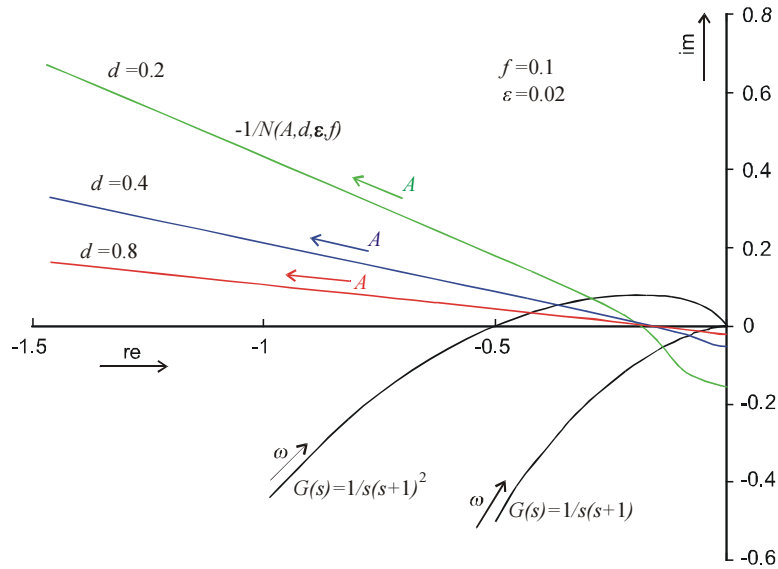
Figure 5: Dependency of $-1/N(A,d,\varepsilon,f)$ on outer relay amplitude d with $\varepsilon = 0.02$

Modification of d results in modifications of the slope in the same way as the previous case (without hysteresis). Equation (4.10) has a physical meaning only for $\varepsilon \le A$. Otherwise the outer relay cannot switch and there are no oscillations. The curves defined by equation (4.10) start in a point given by the condition $A = \varepsilon$. This point is situated on the imaginary axes.

Figure 6 shows the loci of $-1/N(A,d,\varepsilon,f)$ for the equivalent nonlinearity when the outer relay has constant amplitude ($d = const.$) and hysteresis ε varies. The curves $-1/N(A,d,\varepsilon,f)$ shift approximately in vertical sense. Increase of the hysteresis value ε causes the curve $-1/N(A,d,\varepsilon,f)$ to move down (in the vertical sense). This implies that limit cycles frequency decreases.

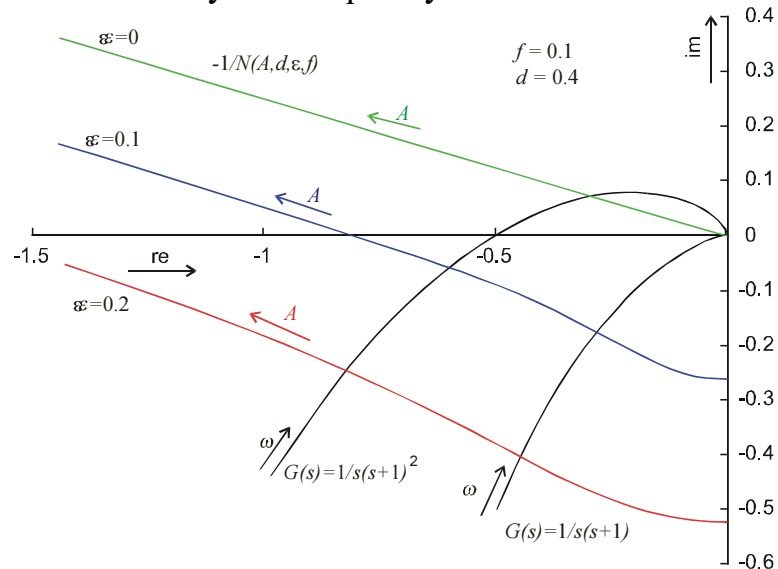*Figure 6: Dependency of $-1/N(A,d,\varepsilon,f)$ on outer relay hysteresis ε with $d = 0.4$*

In short, frequency of limit cycles ω can be modified in two ways:
- by changing outer relay amplitude d, or

- by changing outer relay hysteresis ε.

Each generated limit cycle (intersection between $G(j\omega)$ and $-1/N(A,d,\varepsilon,f)$) can be stable, semi-stable or unstable. It can be shown using extended Nyquist criterion [44] that the intersections in Figure 4, Figure 5 and Figure 6 are all stable.

4.3. Formula for Coulomb Friction Identification

This section presents the derivation of the algorithm for friction identification. When the harmonic balance method is applied to the two-relay system and the outer relay contains non zero hysteresis, condition of harmonic balance can be rewritten as

$$G(j\omega) \cdot N(A,d,\varepsilon,f) = -1 \tag{4.11}$$

Two relay experiments with different settings of the outer relay d and ε can be performed. The following equation then holds to be true for steady state oscillations

$$G(j\omega_1) \cdot N(A_1,d_1,\varepsilon_1,f) = G(j\omega_2) \cdot N(A_2,d_2,\varepsilon_2,f) \tag{4.12}$$

Because the transfer function $G(j\omega)$ is unknown, it would be nice to eliminate it in equation (4.12). Based on the results of section 4.2.3 we assume that it is possible to find different settings of the outer relay parameters (d,ε) resulting in the same frequency of oscillations ω. The equality of frequencies $\omega_1 = \omega_2$ also leads to the equality of complex numbers $G(j\omega_1) = G(j\omega_2)$ and thus simplifying equation (4.12) to

$$N(A_1,d_1,\varepsilon_1,f) = N(A_2,d_2,\varepsilon_2,f) \tag{4.13}$$

Substituting $N(A,d,\varepsilon,f)$ using (4.7) in (4.13) and after some derivations we obtain solution as a complex number with following real and imaginary parts

$$
\begin{aligned}
\bar{f}_{re} &= \frac{1}{A_1 - A_2}\left(\frac{A_1}{A_2}d_2\varepsilon_2 - \frac{A_2}{A_1}d_1\varepsilon_1 \right) \\
\bar{f}_{im} &= \frac{1}{A_1 - A_2}\left(\frac{A_1}{A_2}d_2\sqrt{A_2^2 - \varepsilon_2^2} - \frac{A_2}{A_1}d_1\sqrt{A_1^2 - \varepsilon_1^2} \right)
\end{aligned}
\tag{4.14}
$$

Since $N(A_1,d_1,\varepsilon_1,f)$ and $N(A_2,d_2,\varepsilon_2,f)$ are both approximations of the transfer between e and u, it results that $\bar{f}$ can only yield an approximate value of f. Since f is a strictly real value, we have to look for an approximation of it by a real value. The approximation can be taken either as a real part of $\bar{f}$

$$f = \bar{f}_{re} \tag{4.15}$$

or as its absolute value

$$f = \sqrt{\bar{f}_{re}^2 + \bar{f}_{im}^2}$$

(4.16)

Condition $\bar{f}_{im} \approx 0$ may not always be fulfilled and the ideal solution $f = \bar{f}$ cannot be perfectly obtained. There are two main reasons for this. The first one is caused by the approximative nature of the first harmonic method. In some cases the assumptions on the linear part $G(s)$ are not perfectly fulfilled (linear part must be sufficiently low pass filter which should eliminate all harmonics of the spectrum, except the first harmonics). The second reason is that there are some dynamics between the equivalent nonlinearity and the linear system $G(s)$, denoted by $G_{in}(s)$ and $G_{out}(s)$ in Figure 7. This issue is further discussed in next section.

4.4. Extension of Two Relay System

The real system with friction sometimes differs from the underlying system shown in Figure 1. From this point of view it is interesting to analyze the situation in which the underlying system is enlarged by additional dynamics acting either on the input $G_{in}(s)$ or on the output $G_{out}(s)$ of the linear part (see Figure 7).
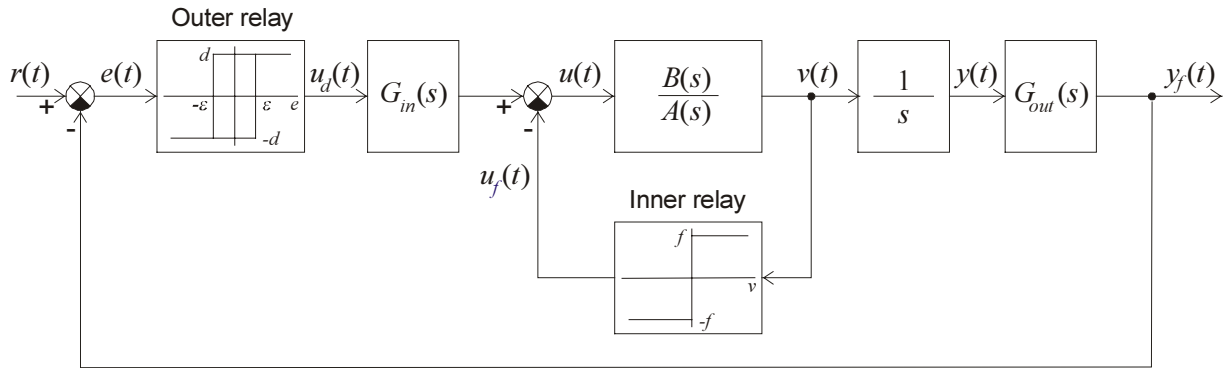
Figure 7: Extended system structure

4.4.1. Input Dynamics G_{in}

The dynamics G_{in} can be included into equivalent nonlinearity. Its describing function is then given by the equation

$$N(A,d,\varepsilon,f) = \frac{4}{\pi A}\left(d \cdot e^{-j\cdot\arcsin\frac{\varepsilon}{A}} + f\frac{1}{G_{in}(j\omega)} \cdot e^{j\cdot\frac{\pi}{2}} \right) G_{in}(j\omega)$$

(4.17)

Using the proposed procedure and from equations (4.13), (4.14) we obtain the solution

$$\bar{f} = \bar{f}_{re} + j \cdot \bar{f}_{im} = f \cdot \frac{1}{G_{in}(j\omega)}$$

(4.18)

The solution is a complex number depending on $G_{in}(j\omega)$. If a non-negligible unknown dynamics is acting on the plant input (actuator dynamics, for example) than it is not possible to use the proposed procedure to compute friction estimate. Moreover, the friction coefficient is dependent on ω and simple model based friction compensator cannot reach its cancellation.

4.4.2. Output Dynamics G_{out}

On the other hand, the dynamics G_{out} connected to the output of linear part changes the describing function of the equivalent nonlinearity to

$$N(A,d,\varepsilon,f)=\frac{4}{\pi A}\left(d\cdot e^{-j\cdot\arcsin\frac{\varepsilon}{A}}+f\cdot e^{-j\angle G_{out}(j\omega)}\cdot e^{j\cdot\frac{\pi}{2}}\right) \qquad (4.19)$$

The additional dynamics G_{out} causes an additional phase shift of the inner relay input $v(t)$ according to output $y_f(t)$. Phase shift changes from $\pi/2$ to $\pi/2$ minus phase shift given by $\angle G_{out}(j\omega)$ (compare (4.19) with (4.7) in the term containing f). Let us substitute $f\cdot e^{-j\angle G_{out}(j\omega)}$ with $\bar{f}$

$$(4.20) \quad \bar{f}=\bar{f}_{re}+j\cdot\bar{f}_{im}=f\cdot e^{-j\angle G_{out}(j\omega)}$$

One can notice that $\left|\bar{f}\right|=f$, i.e. in the ideal case, the absolute value of the solution is the true value f. The outlined procedure can be used and the estimated value of friction is given by the absolute value of the complex number $\bar{f}_{re}+j\cdot\bar{f}_{im}$ computed using (4.16). Our realization uses this equation for computing Coulomb friction estimate to cover both, the simple and the extended cases.

The dynamics G_{out} can be present or included in the system structure due to following reasons:

- It can represent a sensor dynamics or other dynamics on the output of the system.
- It can be added as a filter to reduce the level of noise.
- It can be added as an additional dynamics to more fulfill the requirements of the harmonic balance method when the order of the linear part $G(s)$ is low.

The positive influence of G_{out} has proven itself in the simulations and it real-time application as well.

4.5. Compensation Procedure

Hysteresis adjustment during the second relay experiment is performed using an iterative procedure which behaves like an integral action to reach zero steady state error of the difference between the oscillation frequencies. The integral formula is described by

$$\varepsilon_{2_{i+1}} = \varepsilon_{2_i} + k_\varepsilon A_{2_i} \frac{T_1 - T_{2_i}}{T_{2_i}} \tag{4.21}$$

where k_ε is iteration weighting factor, A_{2_i} is amplitude of system output at i^{th} step, T_1 is stabilized period of oscillations during first relay experiment and T_{2_i} is actual period of oscillations in i^{th} step of the second relay test. The weighting factor k_ε determines the speed of iterations. Higher weighting factor k_ε brings together higher speed of iterations but possibly also more oscillating behavior of ε and consequently of ω and of f. The setting of the weighting factor k_ε is related with oscillation convergence speed.

4.6. Step by Step Description of the Algorithm

The described algorithm can be summarized into the following steps:

First relay test The system is connected in feedback with a relay with hysteresis ε_1 and with amplitude d_1. As soon as the self-oscillations are stabilized, we obtain their frequency ω_1 by measuring their period T_1. The amplitude A_1 of system output is measured too.

Second relay test

Initialization

The amplitude of the outer relay is changed to d_2. The hysteresis of the outer relay is left unchanged $\varepsilon_{2_1} = \varepsilon_1$.

Iteration I

According to the measurement of the oscillation period T_{2_i} and amplitude A_{2_i}, a new value of hysteresis $\varepsilon_{2_{i+1}}$ can be computed using (4.21).

Stop condition

The iterations stop as soon as the current period of the auto-oscillations equals the period obtained during the first relay experiment $T_{2_i} = T_1$ with the relevant precision.

Friction estimation

Equations (4.14) for the real and imaginary part of the solution can be used. The actual value of Coulomb friction is estimated using equation (4.16) as the absolute value of complex number $\bar{f}$.

4.7. Alternative Method

It is well known that the phase shift modification during the relay test can be obtained by adjusting hysteresis value ε of the outer relay and also by adjusting the time delay value τ in a block following the ideal relay [45]. Phase shift modification using adjustable time delay was the motivation to find an alternative method for

Coulomb friction estimation. The basic principle of this alternative method is the same as in the previous case. First, we must find the describing function of new equivalent nonlinearity, i.e. of the system in feedback with an ideal outer relay followed by a block with adjustable time delay τ combined with the inner relay.

The time response of equivalent nonlinearity to harmonic signal is the same as in the case of relay with hysteresis (see Figure 3). The phase shift α_1 is now given by the time delay τ and by the oscillation frequency ω: $\alpha_1 = \omega\tau$. The phase shift $\alpha_2 = \pi/2$ stays the same.

The describing function computed using the first harmonic approximation is given by the sum of two describing functions – of outer relay with phase shift α_1 and of the inner relay with phase shift α_2

$$N(A,d,\omega,\tau,f) = \frac{4}{\pi A}\left(d\cdot e^{-j\cdot\omega\tau} + f\cdot e^{j\cdot\frac{\pi}{2}} \right) \tag{4.22}$$

We assume an equation similar to (4.12)

$$G(j\omega_1)\cdot N(A_1,d_1,\omega_1,\tau_1,f) = G(j\omega_2)\cdot N(A_2,d_2,\omega_2,\tau_2,f) \tag{4.23}$$

Using the same procedure as for the case of the relay with adjustable hysteresis, i.e. eliminating $G(j\omega_1)$ and $G(j\omega_2)$ in equation (4.23) we obtain following expressions for the real and imaginary parts of Coulomb friction estimate $\bar{f}$, respectively

$$\bar{f}_{re} = \frac{1}{A_1 - A_2}\left(A_1 d_2 \sin(\omega_1\tau_2) - A_2 d_1 \sin(\omega_1\tau_1)\right)$$

$$\bar{f}_{im} = \frac{1}{A_1 - A_2}\left(A_1 d_2 \cos(\omega_1\tau_2) - A_2 d_1 \cos(\omega_1\tau_1)\right) \tag{4.24}$$

Formulae (4.24) are mathematically more complex comparing with (4.14) because they contain trigonometric functions. Mathematically higher complexity should not cause problems even when slow hardware or single chip devices without trigonometric function library are used for real time implementation. The reason is that the discussed equations can be used only once and moreover they can be computed off-line. On the other hand, the presence of an ideal relay without hysteresis can cause problems in real applications due to noise in the output signal *y(t)*. The ideal relay would have to be replaced with relay with small hysteresis ($\varepsilon << A$) to eliminate the influence of the noise and to avoid its influence on describing function of equivalent nonlinearity.

The inner relay amplitude estimate is given (as well as for relay with hysteresis) by absolute value (4.16).

For systems with monotonous frequency response $G(j\omega)$, an increase of time delay τ causes decrease of oscillation frequency. The time delay τ can be modified using following iterative algorithm to reach desired frequency of oscillations ω.

$$\tau_{2_{i+1}} = \tau_{2_i} + k_\tau \left(T_1 - T_{2_i}\right)$$ (4.25)

where k_τ is an iteration weighting factor. It specifies the convergence speed, just like the constant k_ε in the case of the relay with hysteresis.

4.8. Influence of Coulomb Friction on Frequency Response Measurement

The describing function in presence of Coulomb friction changes to the form shown in equation (4.7). As it was already pointed out in section 4.2.3, the intersection between the frequency characteristic of $G(s)$ and the negative inverse of describing function $-1/N(A)$ depends on outer relay amplitude d and on Coulomb friction parameter f. Following the intersections depicted in Figure 4, we can state following notice.

The methods for PID controller adjustment based on the results of relay experiment for the systems with friction sometimes give unsatisfactory results. The reason is that these methods do not measure expected critical point with phase shift $-\pi/2$ but the point whose phase shift is lower, depending on the value of outer relay amplitude d. Higher values of d gives the point with phase shift more close to $-\pi/2$, which makes the controller design better.

The control engineer is usually admonished to utilize small values of outer relay amplitudes d not to disturb the system. It is unfortunately in contradiction with last notice.

The situation is the same for the methods requiring point or points with different phase shift. E.g. methods of Landau and Voda [46], [47], [48] and [49] which require the point on frequency response with phase shift $-3\pi/4$. The relay with hysteresis or relay with adjustable time delay is used to measure this point. In both cases, such a measurement does not give correct results due to dependence of describing function on inner and outer relay amplitude. The problem is apparent in view of Figure 5 and Figure 6.

4.9. Simulation Example

Simulations were realized using Matlab 5.2 with Simulink 2.2. We have created some C-mex S-functions because it would be difficult to construct some blocks using supported Simulink blocks.
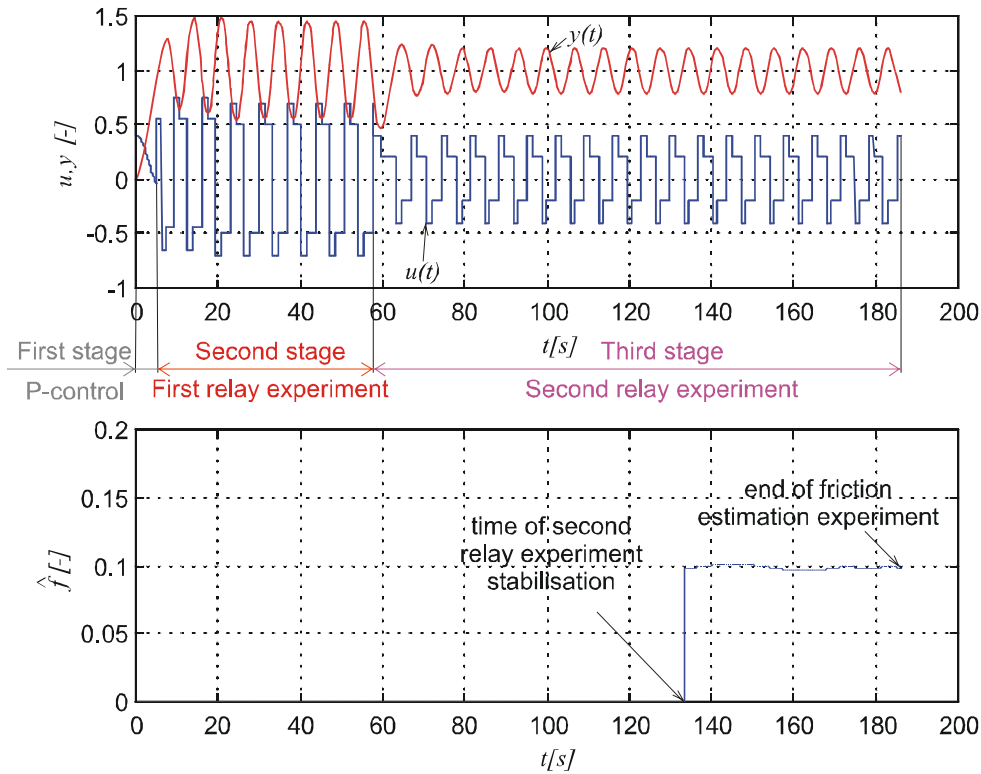
Figure 8: Friction estimation experiment

The simulation scheme (see Figure 9) includes all the steps of the algorithm for friction estimation as presented in section 4.6. Moreover, it contains the P-control stage to lead the system to steady state. This simulation scheme uses conditional and triggered execution of subsystems to realize the outlined algorithm.

4.9.1. More Complex Friction Models

As it was pointed out in section 4.1, the presence of viscous friction does not influence presented algorithm. Situation is the same with stiction. Stiction appears at zero velocity only. The proposed algorithm does not stay in quiet state with zero velocity, it just makes velocity reversals and that's why the stiction is not problematic. Presence of Stribeck effect can cause the increase of Coulomb friction estimate. Especially when the experiment runs on small velocities, because the Stribeck effect is significant there. The solution is to increase the average speed, e.g. by output filtering or by changing the parameters of outer relay.

The hysteresis included in outer relay makes the experiment robust and insensitive to noise disturbances. The proposed algorithm is thus suitable for practical usage.

Description: This scheme identifies the friction which is present in the system. Two relay tests are used to compute value of friction. The equality -1/N(A1) = -1/N(A2) is valid when oscilation of both relay tests have the same frequency i,e, omega1=omega2. Then also N(A1)=N(A2) is valid. Solving this equation we obtain final equation for friction f=1/(A1-A2)*(A1*d2*eps2/A2-A2*d1*eps1/A1) where Ax, dx and epsx are amplitude of oscillation, output amplitude of relay and hysteresis of relay respectively.

You can choose the different friction models and with diferrent initial settings of relays.
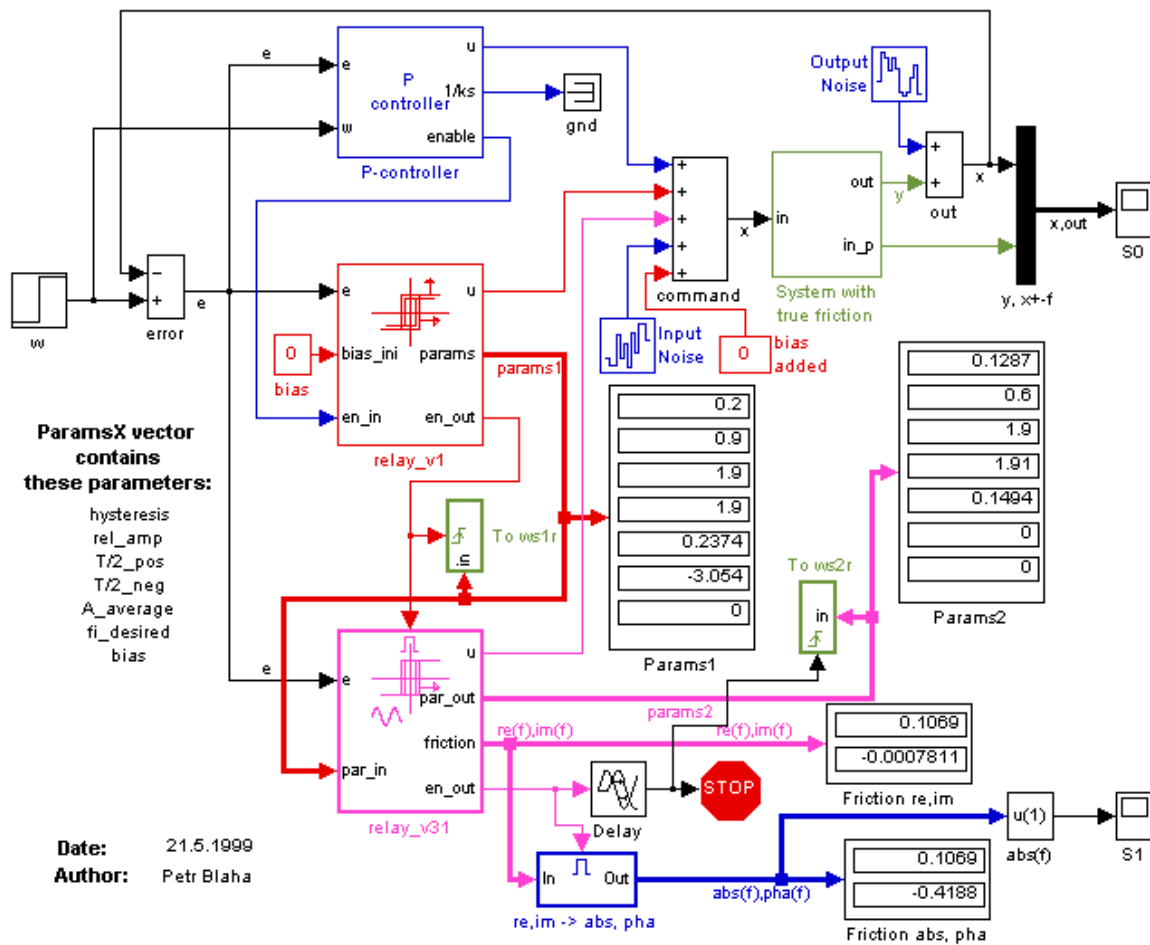
Figure 9: Simulation scheme in Simulink

4.10. Real-Time Experiment

The proposed algorithm was also tested on Coulomb friction identification of DC motor. Its angular velocity was reduced with gear-box. The real-time control was established directly from Simulink environment using real time extension represented by Windows application WinCon 3.0 (Quanser Consulting, Inc.).

The simplified block diagram of DC motor is depicted in Figure 10. The quantity names used in labels are described as follows.

U_{θ_r} ..... reference signal of output shaft position in volts

U_{θ} ...... actual position of output shaft converted to voltage

ω .... angular velocity in *rad/s*

θ_m ...... actual position of DC motor shaft in *rad*

The numerical constants of this system were approximately known. Time constant $\tau = 28 ms$, speed constant $k_{DT} = 8 \cdot 10^3 V/rad/s$ and gearing of the gear-box $1/n = 0.01$. The position was measured by a resistive sensor that transformed the position from the range of $(0, 2\pi) rad$ into voltage in the range of $(-10, 10) V$. The electrical time constant was negligible with respect to the mechanical one and that's why it is not included in the simplified diagram in Figure 10.
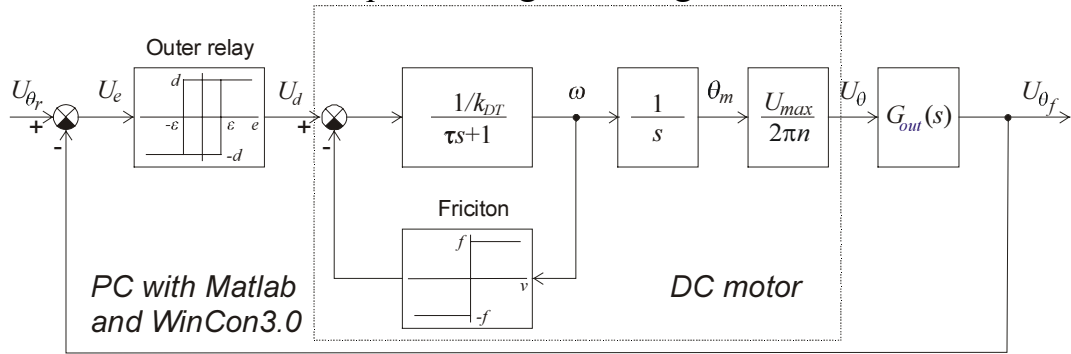
Figure 10: Block diagram of real time experiment with DC motor

It was sufficient to replace the block that contains model of plant with friction nonlinearity with the special block from WinCon 3.0 library containing A/D and D/A modules providing the connection to MultiQ input/output card to be able to run real time experiment.

Figure 11: Results of real-time experiment

Thereafter, the timer module had to be inserted into Simulink scheme. Than it was sufficient to run the compilation, to build the real-time application and to launch real-time experiment.

To obtain better results, we also used a low pass filter with approximately the same dynamics as the system dynamics $G_{out}(s) = 20/(s + 20)$. This modification (as

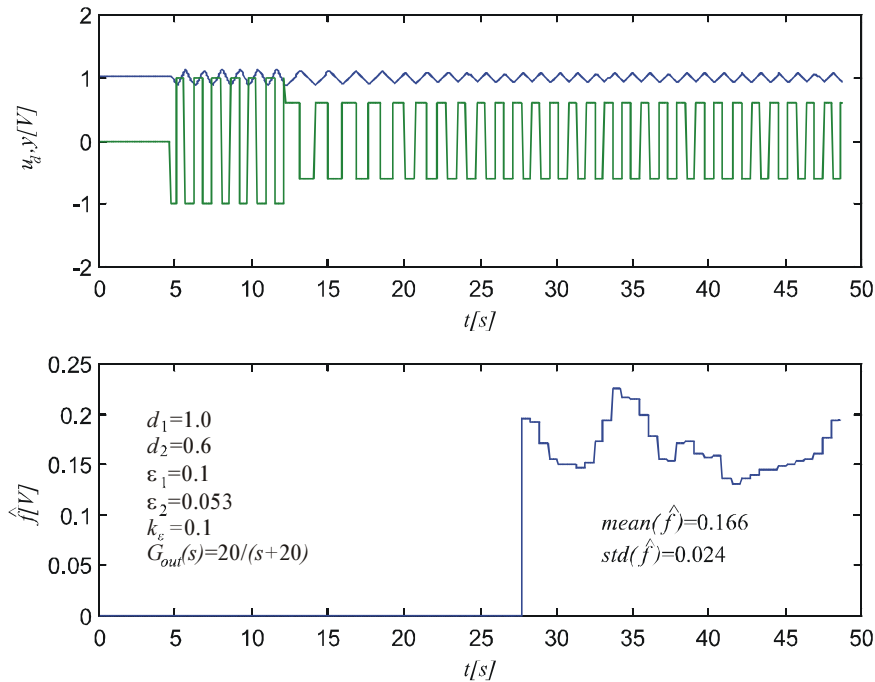well as in simulations) improved the behavior and the obtained results were less varying. The parameters used for obtaining friction estimate are shown directly in Figure 11.

5. CONCLUSION

Dissertation thesis fulfilled the goals traced out in introduction and in objectives. The thesis successfully analyses a two-relay system configuration. The time domain analysis gives some important remarks about the two-relay system. It also shows that no DC component propagates through equivalent nonlinearity. It can be demonstrated by phase plane analysis of linear part of second order with equivalent nonlinearity that some systems converge towards limit cycles faster than the others.

Frequency domain analysis gives the formula for describing function of equivalent nonlinearity. This formula is the milestone of this thesis. It is used to elicit relatively simple formula for inner relay amplitude estimation, which models the Coulomb friction. This formula for Coulomb friction estimation is the main objective of this thesis. Its derivation comes from the dependency of the oscillation period on outer relay amplitude d, hysteresis ε and inner relay amplitude f. The dependency on d and ε is studied in details. The theoretical part in section 4.4 contains also discussion on possible results and the influence of output filtering on estimation results and their precision. It can be declared that this theoretical part described above is original and creates the core of this dissertation thesis.

Simulation examples show "one press button" implementation of the proposed algorithm in Simulink environment of Matlab and some its simulation results. It was observed that the higher order of linear part gives better results due to their better filtering capabilities. The influence of incorporating more complex friction model is described too. It was pointed out that the presence of Stribeck effect can cause increase of Coulomb friction estimate, especially when the system during experiments runs to small velocities.

The presented algorithm for Coulomb friction estimation is implemented as real time application, which was tested on a DC motor. The positive assets of output filtering approved itself.

The advantage of the proposed algorithm is its simplicity to realize it. Another good feature comparing with existing methods for Coulomb friction identification is that it does not require any numerical information about the system to be investigated.

The drawback of this method is long time needed for both relay experiments. We have to wait until the system produces steady state oscillations. Second relay experiment is more time consuming comparing with the first one, because the iterative process of relay parameters changes is used for reaching the same frequency of oscillations as during first relay experiment. This drawback is common for all algorithms where the iteration is engaged.

Presented algorithm can be farther meliorated. The same formula will hold true in a case when phase-locked loop identification will be used at a place of outer relay

feedback. This approach partially removes faults of first harmonic approximation method.

The Coulomb friction estimate obtained using proposed algorithm can be used in existing friction compensators to improve their control performance. It can be also used as a good initial estimate for different adaptive friction compensation methods.

6. ODHAD SUCHÉHO TŘENÍ POUŽITÍM METODY HARMONICKÉ LINEARIZACE SYSTÉMU SE DVĚMA NELINEARITAMI TYPU RELÉ

6.1. Rozšířený abstrakt

Přítomnost nelineárního prvku v řízeném systému často komplikuje život automatizačnímu technikovi, který má takovýto systém řídit. Většinou totiž nemůže použít přímo klasické metody známé pro řízení lineárních systémů, ale musí se buď nejprve vypořádat s nelinearitou, nebo použít speciální návrhové metody.

Jednou z nelinearit, kterou se zabývá tato práce, je mechanické tření. Mechanické tření je složitý fyzikální jev, který nepříjemně ovlivňuje kvalitu regulačního pochodu. Jeho přítomnost v řízeném systému se může projevovat vznikem trvalé ustálené odchylky, nebo vznikem autooscilací kolem žádané hodnoty (tzv. *hunting effect*). To vedlo ke vzniku algoritmů, které nějakým způsobem odstraňují vliv tření. Nejprve vznikaly algoritmy, které nevyžadují znalost modelu. Jedná se o dynamické mazání a omezení zesílení integrátoru. Nevýhodou dynamického mazání je přítomnost vysokofrekvenční složky na výstupu akčního členu vedoucí ke snížení životnosti daného zařízení. Druhá metoda nedosahuje podstatného zvýšení přesnosti řízení. Novější metody kompenzace vycházejí ze znalosti modelu tření. Jedná se o statické modely, které ale nejsou dobré pro rychlosti blízké nule a rovné nule. Nejnovější metody používají dynamické modely, které odstraňují nedostatky modelů statických.

Jednou z nejdůležitějších složek těchto modelů je suché (Coulombovo) tření. V současné době existují metody pro jeho zjištění. Jejich nevýhodou je požadavek na znalost některých parametrů systému, které se musejí nejprve změřit nebo vypočítat a teprve potom lze přistoupit k určení suchého tření. Tato práce popisuje originální algoritmus pro získání odhadu suchého tření u systému, jehož parametry nejsou známé.

Pro matematické odvození algoritmu byla provedena teoretická analýza systému se dvěma nelinearitami typu relé. První nelinearita, nazývaná v této práci jako *vnitřní relé*, má charakteristiku ideálního relé. Tvoří rychlostní zpětnou vazbu a modeluje suché tření. Druhá nelinearita, označovaná v této práci jako *vnější relé*, má charakteristiku relé s hysterezí. Vnější relé tvoří polohovou zpětnou vazbu a zajišťuje vznik autooscilací ve zpětnovazebním systému. Bylo pozorováno, že autooscilace jsou závislé na amplitudách obou nelinearit a na hysterezi vnějšího relé. Toto zjištění bylo motivací pro odvození algoritmu pro odhad amplitudy vnitřního relé, tj. pro odhad suchého tření. Analýza tohoto systému v časové oblasti ukazuje, že v případě ustálených symetrických kmitů je možné obě nelinearity nahradit jednou nelinearitou se stejným chováním – *zástupná nelinearita*. Dá se ukázat, že se systémem nešíří stejnosměrná složka ani v případě, kdy je nenulová žádaná hodnota.

Podmínky pro vznik a stabilitu autooscilací se dají u systémů s lineární částí druhého řádu ukázat pomocí metody izoklin a Poincaré-Bendinxsonova teorému .

Výsledky zjištěné analýzou v časové oblasti umožňují použít metodu harmonické rovnováhy a provedení analýzy ve frekvenční oblasti. Nejprve je zjištěn ekvivalentní přenos zástupné nelinearity. Ten je rozebrán z hlediska závislosti na amplitudě a na hysterezi vnějšího relé. Existenci a stabilitu autooscilací je možné určit použitím modifikovaného Nyquistova kritéria. Na základě znalosti ekvivalentního přenosu je použitím metody harmonické rovnováhy odvozen vzorec a sestaven algoritmus pro určení odhadu suchého tření. Navržená metoda a její teoretické odvození je původní a tvoří jádro těchto tezí.

Vzniklý algoritmus je realizován v prostředí Simulinku v programu Matlab. Některé jeho bloky jsou naprogramovány jako S-funkce v jazyce C. Pomocí toolboxu Real Time Workshop a aplikace WinCon 3.0 lze vygenerovat aplikaci, která běží v reálném čase. Algoritmus byl ověřen při zjišťování suchého tření stejnosměrného motorku.

Práce byla částečně publikována na konferenci PID2000, která se konala ve Španělském městě Terrassa. Dále byla zaslána a předběžně přijata do časopisu Control Engineering Practice.

6.2. Nástin odvození algoritmu

Při odvození algoritmu uvažujeme systém podle Obr. 1. Toto zapojení se dá na základě analýzy v časové oblasti za předpokladu symetrických ustálených kmitů a konstantního řízení $w(t) = konst.$ zjednodušit na zapojení viz. Obr. 2. Přenos lineární části obvodu je $G(p) = B(p)/p \cdot A(p)$. Na toto zapojení již lze použít metodu harmonické rovnováhy. Prvním krokem harmonické rovnováhy je určení ekvivalentního přenosu zástupné nelinearity.
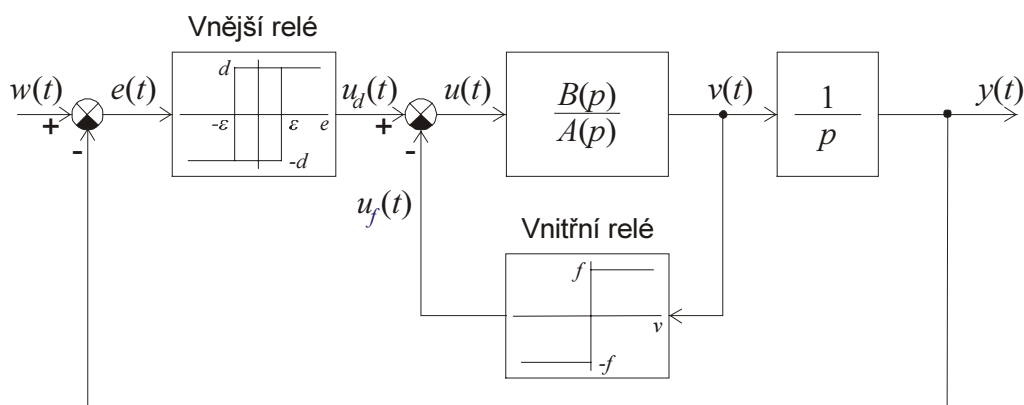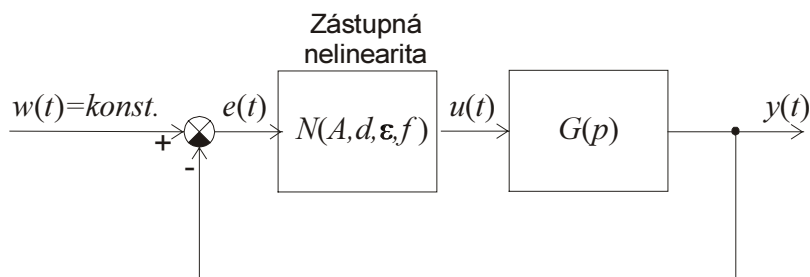

Obr. 1: Základní schéma zapojení

Pro zjištění ekvivalentního přenosu je třeba znát odezvu nelinearity na harmonický signál $e(t) = A \cdot \sin(\omega t)$. Tato odezva se skládá z rozdílu dvou vzájemně posunutých obdélníkových signálů $u_d(t)$ a $u_f(t)$ (viz. Obr. 3). Výstup vnějšího relé

je z důvodu hystereze ε posunut vůči uvažovanému harmonickému signálu $e(t)$ o úhel $\alpha_1 = \arcsin(\varepsilon/A)$. Výstup vnitřního relé je posunut vůči $e(t)$ o úhel $\alpha_2 = \pi/2$.

Vzorec pro výpočet ekvivalentního přenosu zástupné nelinearity má tvar

$$N(A,d,\varepsilon,f) = \frac{4}{\pi A}\left(d \cdot e^{-j\cdot\alpha_1} - f \cdot e^{-j\cdot\alpha_2}\right) = \frac{4}{\pi A}\left(d \cdot e^{-j\cdot\arcsin\frac{\varepsilon}{A}} + f \cdot e^{j\cdot\frac{\pi}{2}}\right) \quad (6.1)$$

Obr. 2: Zjednodušené schéma zapojení

Předpokládejme, že provedeme dva experimenty s různým nastavením parametrů vnějšího relé. Potom na základě podmínky pro existenci ustálených kmitů v uzavřeném obvodu $G(j\omega) \cdot N(A,d,\varepsilon,f) = -1$ platí následující vztah

$$G(j\omega_1) \cdot N(A_1,d_1,\varepsilon_1,f) = G(j\omega_2) \cdot N(A_2,d_2,\varepsilon_2,f) \quad (6.2)$$

Protože přenos lineární části $G(j\omega)$ není známý, je nutné ho z výše uvedené rovnice odstranit. Dá se ukázat, že frekvence ustálených kmitů se dá ovlivnit změnou parametrů vnějšího relé, tedy změnou jeho amplitudy d a hystereze ε. Dále se dá ukázat, že mohou existovat dvě různá nastavení parametrů d_1, ε_1 a d_2, ε_2, při kterých systém vykazuje autooscilace na stejné frekvenci $\omega_1 = \omega_2$. Potom se rovnice (6.2) zjednoduší na tvar

$$N(A_1,d_1,\varepsilon_1,f) = N(A_2,d_2,\varepsilon_2,f) \quad (6.3)$$

Dosazením (6.1) do (6.3), postupným zjednodušením a vyjádřením parametru f dostaneme vzorec pro výpočet jeho reálné a imaginární složky

$$\bar{f}_{re} = \frac{1}{A_1 - A_2}\left(\frac{A_1}{A_2}d_2\varepsilon_2 - \frac{A_2}{A_1}d_1\varepsilon_1\right)$$

$$\bar{f}_{im} = \frac{1}{A_1 - A_2}\left(\frac{A_1}{A_2}d_2\sqrt{A_2^2 - \varepsilon_2^2} - \frac{A_2}{A_1}d_1\sqrt{A_1^2 - \varepsilon_1^2}\right) \quad (6.4)$$

Odhad velikosti suchého tření se dá určit ze vzorce (6.4) buďto jako reálná část, nebo jako absolutní hodnota. Imaginární část by totiž měla být teoreticky rovna nule. To často zcela neplatí z důvodu použití přibližné metody. Popsané schéma může být

rozšířeno o výstupní filtr s přenosem $G_{out}(s)$. To způsobí pouze změnu fáze v odhadu $\bar{f}$, neovlivní to však jeho amplitudu. To je důvod, proč v našem algoritmu používáme odhad velikosti suchého tření f jako absolutní hodnotu komplexního čísla (6.4).

$$f = \sqrt{\bar{f}_{re}{}^2 + \bar{f}_{im}{}^2} \qquad (6.5)$$
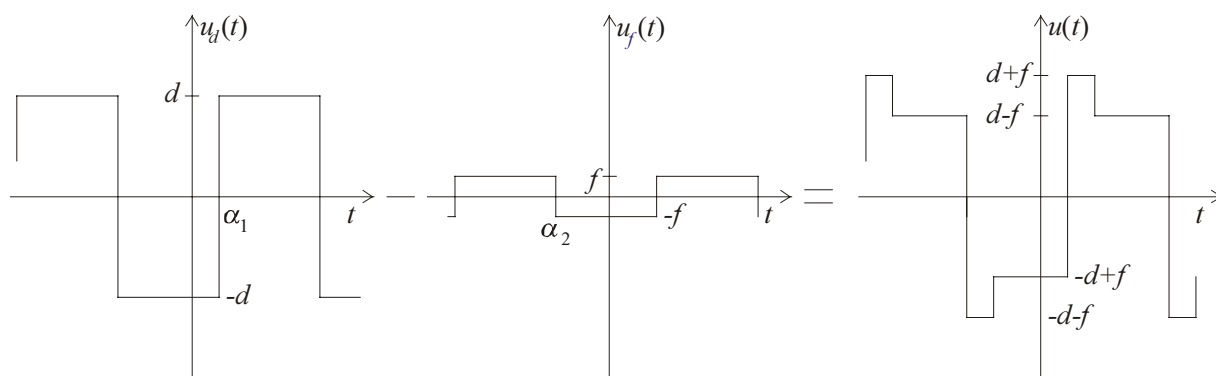
Obr. 3: Odezva zástupné nelinearity na harmonický signál

Pro zajištění rovnosti frekvencí během obou experimentů je navržen iterativní algoritmus nastavující velikost hystereze vnějšího relé podle vzorce

$$\varepsilon_{2_{i+1}} = \varepsilon_{2_i} + k_\varepsilon A_{2_i} \frac{T_1 - T_{2_i}}{T_{2_i}} \quad , \qquad (6.6)$$

kde T_1 je perioda autooscilací během prvního experimentu a T_{2_i} je perioda autooscilací v daném iteračním kroku. Konstanta k_ε určuje rychlost konvergence. Správná konvergence byla dosažena pro hodnoty tohoto parametru v rozmezí (0.01,0.1).

6.2.1. Alternativní metoda

Existuje také alternativní metoda, která pro vytvoření autooscilací nepoužívá nelinearitu typu relé s hysterezí, ale nelinearitu typu ideálního relé s proměnným dopravním zpožděním τ. Vzorec pro výpočet ekvivalentního přenosu zástupné nelinearity s dopravním zpožděním

$$N(A, d, \omega, \tau, f) = \frac{4}{\pi A}\left(d \cdot e^{-j \cdot \omega \tau} + f \cdot e^{j \cdot \frac{\pi}{2}} \right) \qquad (6.7)$$

Alternativní vzorec pro výpočet tření

$$\bar{f}_{re} = \frac{1}{A_1 - A_2}\left(A_1 d_2 \sin(\omega_1 \tau_2) - A_2 d_1 \sin(\omega_1 \tau_1) \right)$$

$$\bar{f}_{im} = \frac{1}{A_1 - A_2}\left(A_1 d_2 \cos(\omega_1 \tau_2) - A_2 d_1 \cos(\omega_1 \tau_1) \right) \qquad (6.8)$$

Odhad suchého tření se provádí stejně jako v minulém případě, tedy jako absolutní hodnota komplexního čísla (6.8) podle vzorce (6.5). Iterace pro nastavení dopravního zpoždění v následném iteračním kroku (periodě autooscilací) se provádí podle vzorce

$$\tau_{2_{i+1}} = \tau_{2_i} + k_\tau \left(T_1 - T_{2_i} \right) \tag{6.9}$$

Konstanta k_τ určuje opět rychlost konvergence.

6.3. Stručný popis algoritmu

Popsaný algoritmus může být shrnut do následujících kroků:

První experiment

Systém se zapojí do zpětnovazebního obvodu s relé s hysterezí ε_1 a s amplitudou d_1. Jakmile se autooscilace ustálí, změří se jejich perioda T_1 a amplituda A_1.

Druhý experiment

Inicializace

Amplituda vnějšího relé se změní na hodnotu d_2. Jeho hystereze se ponechá na původní hodnotě $\varepsilon_{2_1} = \varepsilon_1$.

Iterace i

Podle změřené hodnoty periody autooscilací T_{2_i} a hodnoty jejich amplitudy A_{2_i} se pomocí vzorce , (6.6) nastaví nová velikost hystereze $\varepsilon_{2_{i+1}}$.

Podmínka ukončení algoritmu.

Iterace se ukončí v okamžiku, kdy se perioda kmitů T_{2_i} shoduje s periodou kmitů T_1 získanou při prvním experimentu $T_{2_i} = T_1$.

Výpočet odhadu tření.

Vypočte se odhad velikosti suchého tření použitím vzorců (6.5) a (6.4).

6.4. Závěr

Práce se zabývá metodou automatického zjišťování suchého tření, která pro svoji činnost nevyžaduje číselné informace o měřeném objektu. Jediným požadavkem je, aby se jeho struktura shodovala s uvažovanou strukturou použitou při odvození této metody. Jádro disertační práce tvoří ideový návrh, teoretické odvození a praktická realizace výše popsané metody. Ta byla odzkoušena v simulacích a následně potom na praktickém příkladě odhadu suchého tření stejnosměrného motorku. V práci je ukázána možnost použití filtrace výstupní veličiny. To zvyšuje přesnost navržené metody a umožňuje dosažení lepších výsledků v případě zašuměného obvodu.

7.   VERSION ABRÉGÉE

Cette thèse s'intéresse à l'étude d'un système comportant une partie linéaire et deux parties non-linéaires avec la caractéristique du relais. La non-linéarité intérieur (relais intérieur) a la caractéristique du relais idéal. Ce relais représente le frottement de Coulomb. La non-linéarité extérieure (relais extérieure) créé l'auto oscillation dans la boucle fermée. Il contient un hystérésis.

Les deux relais peuvent être remplacés par un élément non-linéaire avec un comportement identique. Cela permet d'utiliser la méthode appelée : la méthode d'équilibre des harmoniques / analyse de la fonction de description L'amplitude et la fréquence des auto-oscillations dépendent des paramètres du relais extérieure (l'hystérésis et l'amplitude) Cela permet de déduire la formule et l'algorithme pour l'estimation du frottement.

Tout d'abord, les limites du cycle sont générées dans un système utilisant un relais extérieure avec l'hystérésis et l'amplitude fixe. On mesure l'amplitude et la fréquence aussitôt que la limite du cycle est stabilisée. Ensuite, on change la valeur de l'amplitude du relais extérieure. La limite du cycle est générée de nouveau. On augmente la valeur de l'hystérésis pour obtenir la même fréquence que celle du cycle durant le premier test du relais. On mesure l'amplitude du cycle pour la deuxième fois. Finalement, les données obtenues sont utilisées pour le calcul du frottement de Coulomb.

L'algorithme qui est décrit ici a été réalisé sous la forme d'un schéma sous Simulink avec plusieurs C MEX S fonctions sous Matlab. Le schéma a été vérifié par des simulations aussi bien qu'en situations réelles. Le code C a été automatiquement généré par l'outil Real Time Workshop lequel peut être compilé en utilisant le compilateur et logiciel WinCon 3.0. Le fonctionnement en temps réel a été démontré par l'estimation du frottement de Coulomb du moteur à courant continu.

8. REFERENCES

[1] Altpeter, F., Ghorbel, F., Longchamp, R. Relationship between friction models: A singular perturbation. *37*[th] *Conference on Decision and Control*, Tampa, Florida, 1998, p.1572-1574.

[2] Armstrong-Hélouvry, B., Dupont, P. Friction modelling for control. *In 1993 American Control Conf. (ACC '93)*, 1993, p. 1905–1909.

[3] Armstrong-Hélouvry, B., Dupont, P., Canudas de Wit, C. A survey of models, analysis tools and compensation methods for the control of machines with friction. *Automatica*, 1994, vol. 30, no. 7, p. 1083–1138.

[4] Åström, K., Hägglund, T. *Automatic Tuning of PID Controllers*. I.S.A., Research Triangle Parc, 1988.

[5] Åström, K., Hägglund, T. Automatic tuning of simple regulators with specifications on phase and amplitude margins. *Automatica*, 1984, vol. 20, no. 5, p. 645 – 651.

[6] Atherton, D. *Nonlinear Control Engineering*. 1st ed. London, UK, Van Nostrand Reinhold Co. Ltd., 1975.

[7] Bai, E. W. Parametrization and adaptive compensation of friction forces. *Int. Journal of Adaptive Control and Signal Processing (IJACSP)*, 1997, vol. 11, p. 21–31.

[8] Bai, M., Zhou, D. H., Schwarz, H. Identification of generalized friction for an experimental planar two-link flexible manipulator using strong tracking filter. *IEEE Transactions on Robotics and Automation*, 1999, vol. 15, no. 2, p. 362–369.

[9] Balara, D., Žilková, J. The speed-sensorless parametric identification of the nonlinear DC motor with thyristor converter using neural networks. In proc. of Int. Conf. on Artificial Neural Networks and their Application Possibilities, Košice, 1996, p. 50–54.

[10] Besançon-Voda, A. Identification of coulomb friction by two-relay system analysis. *Technical report 96050*, LAG-INPGrenoble, February 1996.

[11] Besançon -Voda, A., Besançon, G. Analysis of a class of two-relay systems - application to coulomb friction identification. *Automatica*, 1996, vol. 35, no. 8, p. 1391–1399.

[12] Besançon -Voda, A., Roux-Buisson, H. Another version for the feedback relay experiment. *Journ. of Process Control*, 1997, vol. 2, no. 7, p. 240–246.

[13] Canudas de Wit, C. Control of friction-driven systems. *In 5*[th] *European Control Conference (ECC '99)*, Karlsruhe, Germany, 1999.

[14] Canudas de Wit, C., Åström, K. J., Braun, K. Adaptive friction compensation in DC-motor drives. *IEEE Journal of Robotics and* Automation, 1987, vol. RA-3, no. 6, p. 681–685.

[15] Canudas de Wit, C., Lischinsky, P. Adaptive friction compensation with dynamics friction model. *13*[th] *Triennial World Congress*, San Francisco, CA, 1996, p. 197–202.

[16] Canudas de Wit, C., Lischinsky, P. Adaptive friction compensation with partially known dynamic friction model. *Int. Journal of Adaptive Control and Signal Processing (IJACSP)*, 1997, vol. 11, p. 65–80.

[17] Canudas de Wit, C., Noël, P., Aubin, A., Brogliato, B. Adaptive friction compensation in robot manipulators: Low velocities. *The International Journal of Robotics Research*, 1991, vol. 10, no. 3, p. 189–199.

[18] Canudas de Wit, C., Olsson, H., Åström, K., Lischinsky, P. A new model for control of systems with friction. *IEEETAC*, 1995, vol. 40, no. 3, p. 419–425.

[19] Cebulski, B., Hofmann, W. Fuzzy-control of mechanical systems with nonlinear friction. *EUFIT '94 - First European Congres on Fuzzy and Intelligent Technologies*, Aachen, Germany, 1994, p. 577–581.

[20] Cho, S. I., Ha, I. J. A learning approach to stick-slip friction compensation. *14*[th] *IFAC World Congress*, Beijing, P.R. China, 1999, p. 169–174.

[21] Colhour, T. G., Nair, S. S. Accurate estimation of friction. *American Control Conference*, Baltimore, Maryland, 1994, p. 1188–1189.

[22] Colombi, S. Comparison of different control strategies and friction compensation algorithms in position and speed control. *IFAC Motion Control 1995*, Munich, October 1993, p. 173–180.

[23] Elhami, M. R., Brookfield, D. J. Sequential identification of coulomb and viscous friction in robot drives. *Automatica*, 1997, vol. 33, no. 3, p. 393–401.

[24] Friedland, B. Aspects of traction control. *Proceedings of the 7th Mediterranean Conference on Control and Automation*, Haifa, Israel, 1999, p. 1261–1271.

[25] Friedland, B., Park, Y. J. On adaptive friction compensation. *IEEE Transactions on Automatic Control*, vol. 37, no. 10, p. 1609–1612.

[26] Gäfvert, M., Svensson, J., Åström, K. Friction and friction compensation in the furuta pendulum. *5th European Control Conference (ECC 99)*, Karlsruhe, Germany, 1999, p. 0–1.

[27] Hamiti, K. *Etude et mise en oeuvre de lois de commande numérique sur un actionneur électro-pneumatique avec frottements*. PhD thesis, Université Joseph Fourier de Grenoble, 1996.

[28] Hang, C., Åström, K., Ho, W. Relay auto-tuning in the presence of static load disturbance. *Automatica*, 1993, vol. 29, no. 2, p. 563 – 564.

[29] Hensen, R. H. A., Angelis, G. Z., van de Molengraft, M. J. G., de Jager, A. G., Kok, J. J. Grey-box modelling of friction: An experimental case study. *5th European Control Conference (ECC '99)*, Karlsruhe, Germany, 1999.

[30] Hsich, C., Pan, Y. C. Sensor-accuracy precision possitioning with the existence of static friction part i - dynamic model of friction during the pre-sliding range. *14th IFAC World Congress*, Beijing, P.R. China, 1999, p. 215–220.

[31] Hsich, C., Pan, Y. C. Sensor-accuracy precision possitioning with the existence of static friction part ii - parameter estimation of static friction and integral control for practical positioning problems. *14th IFAC World Congress*, Beijing, P.R. China, 1999, p. 221–226.

[32] Isermann, R. Towards intelligent control of mechanical processes. *Control Engineering Practice*, 1993, vol. 1, no. 2, p. 233–252.

[33] Jee, S., Koren, Y. A self-organizing fuzzy logic control for friction compensa-tion in feed drives. *American Control Conference,* Seattle, Washington, 1995, p. 205–209.

[34] Karnopp, D. Computer simulation of stick-slip friction in mechanical dynamic systems. *ASME J. of Friction and Wear*, 1985, vol. 107, no. 1, p. 100–103.

[35] Khalil, H. *Nonlinear systems*. 2nd ed. Upper Saddle River, NJ 07458, Prentice-Hall, 1996.

[36] Kim, J. H., Kim, K. C., Chong, E. K. P. Fuzzy precompensated PID controllers. *IEEE Transactions on Control System Technology*, 1994, vol. 2, no. 4, p. 406–411.

[37] Kopacek, P., G. Krenn, T. K., Wernstedt, J. Optimal fuzzy control design for robotics. *39th Internationales Wissenschaftliches Kolloquium*, Illmenau, Ger-many, 1994, p. 301–307.

[38] Koskinen, H. A fuzzy pid-controller for active magnetic bearings. *EUFIT '93 - First European Congres on Fuzzy and Intelligent Technologies*, Aachen, Germany, 1993, p. 1169–1174.

[39] Kristinsson, K., Dumont, G. A. System identification and control using genetic algorithms. *IEEE Transactions on Systems*, Man. and Cybernetics 1992, vol. 22, no. 5, p. 1033–1046.

[40] Layne, J. R., Passino, K. M., Yurkovich, S. Fuzzy learning control for anti-skid braking system. *31st Conference on Decision and Control*, Tucson, Arizona, 1992, p. 2523–2528.

[41] Liang, J. W., Feeny, B. F. Identifying coulomb and viscous friction from free vibration decrements. *Nonlinear Dynamics*, 1998, vol. 16, p. 337–347.

[42] Linden, G. W., Lambrechts, P. F. H_∞ control of an experimental inverted pendulum with dry friction. *IEEE Control Systems Magazine*, 1993, p. 44–50.

[43] Ostergat, E., Carvalho-Ostertag, M. J. Practical experience with fuzzy logic control. *EUFIT '93 - First European Congres on Fuzzy and Intelligent Technologies*, Aachen, Germany, 1993, p. 789–793.

[44] Slotine, J.-J., Li, W. *Applied nonlinear control*. 2nd ed. Englewood Cliffs, New Jersey, Prentice-Hall, 1991.

[45] Tsypkin, J. *Relay control systems*. Cambridge, U.K., Cambridge Univ. Press, 1984.

[46] Voda, A., Landau, I. Applications of the KLV method for the Auto-Calibration of PID controllers. *2nd IEEE Conference on Control Applications (CCA)*, Vancouver, British Columbia, September 1993, p. 829 – 834.

[47] Voda, A., Landau, I. Industrial evaluation of the KLV method for the autocalibration of PID controllers. *1994 IEEE Conference on Control. (IEE 94)*, Coventry, UK, March 1994.

[48] Voda, A., Landau, I. The auto-calibration of PI controllers based on two frequency measurements. *Int. Journal of Adaptive Control and Signal Processing (IJACSP)*, 1995, vol. 9, no. 5, p. 395–421.

[49] Voda, A., Landau, I. A method for the auto-calibration of PID controllers. *Automatica*, 1995, vol. 31, no. 1, p. 41–53.

[50] Šolc, F. *Theory of the automatic control II*. 2nd ed. Czech republic, VUT Brno, 1990.

[51] Šolc, F. Friction modelling and compensation. *MOSIS '98*, Sv. Hostýn, Czech Republic, 1998, p. 91–95.

[52] Ziegler, J., Nichols, N. Optimum settings for automatic controllers. *American Society of Mechanical Engineering Transactions*, 1942, vol. 64, no. 5, p. 759 –768.

9. CURRICULUM VITAE

Petr BLAHA

Krátká 481
Olešnice
679 74
CZECH REPUBLIC

Phone: 0605/722666
E-mail: blahap@yahoo.com
Homepage: www.geocities.com/blahap

Personal

- Nationality: Czech

- Date of birth: 20.8.1973

- Place of birth: Boskovice

- Marital status: single

Education

- 1996 - 1999   Doctoral study on Technical University of Technology in Brno, Faculty of Electrical Engineering and Computer Science, Department of Control and Instrumentation.
  Still unfinished.

- 1991 - 1996   Master degree in automation and control on Technical University of Technology in Brno, Faculty of Electrical Engineering and Computer Science. Department of Control and Instrumentation.
  Dean's award prize for master thesis.

- 1987 - 1991   Secondary technical school Jedovnice, emphasised on automation of processes.

Professional experiences

- spring 1999   four-month stage in France on Ecole Nationale d'Ingenieurs Electrotricien de Grenoble. Programming in real time environment of Matlab and Simulink. Programming in C++.

- spring 1996   four month stage in France on Ecole Superieure d'Ingenieurs an Electrotechnique et Electronique in Paris. Work on master thesis with title: *Implementation of GSM HR speech coder on TMS320C30.*

Languages

English – very good in both writing and speaking

French – passive knowledge

Interests

Sport   – volleyball, football, body building, skiing

Music   – accordion, guitar, flute

Military service

4.10.1999 – 14.9.2000 Military academy in Vyškov

Professional formalisation certificate – supervisor of computer classroom, teacher of informatics (OS Windows 9x, MS Office 97), DTP*.*

10. LIST OF PUBLISHED ARTICLES

[1] Besançon-Voda, A., Blaha, P. Relay Feedback Experiment for Coulomb Friction Identification. *IFAC Workshop on Digital Control - PID2000*, Terrassa (Spain), pp. 335-340, 2000.

[2] Blaha, P., Besançon-Voda, A. Some Aspects of Coulomb Friction Estimation using harmonic Balance Method. *The 13th International Conference on Process Control*, Štrbské Pleso, 2001. Accepted for publication.

[3] Besançon-Voda, A., Blaha, P. Describing Function Approximation of a Two-relay Systems Configuration with Application to Coulomb Friction Identification. *Control Engineering Practice*, 2001. Conditionally accepted for publication.

[4] Pivoňka, P., Blaha, P. Comparative Analysis of Classical and Fuzzy PID Control Algorithms. *7th Zittau Colloquium*, pp. 176-181, Zittau 1999.

[5] Pivoňka, P., Stavěl, J., Blaha, P. Development Tool for Implementation of Intelligent Controllers in Real Processes. *5th Zittau Colloquium*, pp. 83-87, Zittau 1997.

[6] Blaha, P., Pivoňka, P. Intelligent Corrector for the Systems with Time Delay. *42nd International Scientific Colloquium*, pp. 637-641, Ilmenau 1997.

[7] Baudoin, G., Blaha, P. Development of low bit rate speech coder based on the Half Rate GSM standard on a TMS320C30 DSP. *The First European DSP Education and Research Conference*, pp. 1-8, ESIEE Paris 1996.